The Northeast Greenland shelf as a potential late-summer CO_2 source to the atmosphere

Esdoorn Willcox[1], Marcos Lemes[1], Thomas Juul-Pedersen[3], Mikael Kristian Sejr[4], Johnna Michelle Holding[4], and Søren Rysgaard[2]

[1]Centre for Earth and Observation Science, University of Manitoba, Manitoba, Canada
[2]Arctic Research Centre, Aarhus University, Aarhus, Denmark
[3]Pinngortitaleriffik, Greenland Institute of Natural Resources, Kivioq 2, PO Box 570, 3900 Nuuk, Greenland
[4]Institut for ecoscience, Aarhus University, Aarhus, Denmark

Abstract. The Northeast Greenland shelf is a region currently considered to be an annual net sink of carbon dioxide (CO_2) from the atmosphere. Water from the Northeast Greenland shelf is advected to the formation regions of North Atlantic Deep Water and therefore any carbon uptake may be stored for ocean thermohaline circulation timescales. We present the most extensive study of carbon chemistry on the Northeast Greenland shelf to date made possible by opportunistic sampling due to a sudden decrease in sea ice concentration in late August and September 2017. These are the first full-depth measurements of total alkalinity and dissolved inorganic carbon at latitudes between 75 and 79 °N with additional data collected in the region of the Northeast Water Polynya and outside Young Sund. We find that surface mixed layer concentrations are variable and for many stations higher than the interpolated atmospheric concentration for the region during the sampling period. Below the surface mixed layer, CO_2 concentrations increase linearly with decreasing apparent oxygen utilisation. The mixed layer deepens during the study period which is associated with apparent changes in CO_2 uptake. The Northeast Greenland shelf is a hydrologically complex region with many processes influencing the carbonate system at smaller scales than our sampling density. The scatter in the dataset are more than mere outliers and their lack of relationship to any measured variable indicates a strong influence of currently undescribed process(es) or variable(s) at the sampled scales. These data were collected during a time of radically low sea ice concentrations for the region and may be an indication of future conditions. Since they indicate the potential of the region to act as a seasonal source of CO_2 to the atmosphere this may modify our current estimate of the region as a strong annual net sink relatively protected from the immediate influence of atmospheric warming and climate change.

1 Introduction

The Arctic Ocean and adjecent continental shelves are changing rapidly under the influence of climate change (Serreze and Barry, 2011; Richter-Menge et al., 2017; Overland et al., 2019; Stroh et al., 2019). The Northeast Greenland shelf is an Arctic outflow shelf (Carmack and Wassmann, 2006; Michel et al., 2015) and one of the two gateways (the other the Canadian Arctic Archipelago) through which water from the Arctic Ocean is transported southward into the North Atlantic Ocean (Hunt et al., 2016). Together with the along-slope East Greenland Current (EGC), the shelf acts as a gateway through which water from the Arctic Ocean can be advected to the Greenland Sea, the Irminger Sea, and the Labrador Sea, regions that are crucial to the Atlantic Meridional Overturning Circulation through the formation of intermediate and deep water masses (Smethie and Fine, 2001). This means that any carbon stored in the region may be retained in the global oceans on the timescales of the thermohaline circulation (Broecker, 1997; Farmer et al., 2019). The consensus is that the Northeast Greenland shelf has been a net annual carbon sink like other Arctic shelf regions, though this appears to be changing in response to changing conditions. The initial determination of the region as a sink was made through interpolation studies (Takahashi et al., 2014), Self Organising Maps (SOM, Yasunaka et al. (2018)), and temporally and/or spatially limited observations using various methods, most focused on the Northeast Water Polynya or the near-coastal regions and fjords (Yager et al., 1995; Nakaoka et al., 2006; Sejr et al., 2011; Bakker et al., 2023). Recent studies have indicated the potential for the region to become corrosive in terms of aragonite saturaton (Fransson et al., 2023) and highlight the difference between the carbon system on the eastern side of Greenland versus the west in terms of the relationship between carbon chemistry and depth (Henson et al., 2023, 2024). The latter is far more pronounced in western than eastern shelf areas and may be related to differences in their respective hydrography. Higher benthic production nearer to the shelf edge may be indicative of stronger primary productivity in this area, though the shelf is considered to be oligotrophic and the previously strong benthic-pelaic coupling in the region may be weakening (Bodur et al., 2024). Due to high sea ice cover during all seasons the shelf is challenging to access, making it difficult to consistently measure all the parameters required to determine the conditions and processes influencing dissolved CO_2 concentrations.

The northern North Atlantic and the Greenland Sea are more accessible and studies in these regions receiving water from the Northeast Greenland shelf and EGC (e.g. Olsen et al. (2008), Olafsson et al. (2021)) show that waters sourced from the Arctic remain undersaturated in dissolved CO_2 while Atlantic waters can act as a weak seasonal source. Water from the North Atlantic that might be entrained into the EGC also tends to be undersaturated (Jones et al., 2021; Ericson et al., 2023), but has rapidly increasing concentrations, particularly in Autumn below latitudes of 78 °N when concentrations are at or near that of the atmosphere.

The uptake of CO_2 gas from the atmosphere in the northern North Atlantic (>50 °N) is partially driven by the cooling of warm water at the surface during northward transport which increases gas solubility, including CO_2. High stratification and primary productivity in summer combined with deep convective mixing in winter enable the exposure of a more water to the atmosphere which further facilitates uptake. The Arctic Ocean carbon system is less well understood due to low (spatial and temporal) sampling densities though the Eurasian Basin uptake of anthropogenic CO_2 is thought to be increasing (Rajasakaren et al., 2019). There are also additional processes at play in northern latitudes that influence CO_2 gas exchange, affecting both the solubility and biological pumps in the region such as the sea ice related processes of brine expulsion and sea ice melting, and the input of 10-11% of global meteoric river water (Shiklomanov et al., 2021). Each of these is characterised by their seasonality (Bates et al., 2009; von Appen et al., 2021). The Atlantic Water being transported north into the Arctic (and into the EGC as part of the return Atlantic Current) is much warmer than it was in previous decades (Polyakov et al., 2017). This increase in heat has been associated with changes in the Arctic halocline which shields sea ice from melting from below (Polyakov et al., 2020) and is likely to also stimulate heating in the EGC and potentially the Northeast Greenland shelf where the warm surface water from the return Atlantic Current (RAC) comes in direct contact with sea ice advected from the Arctic Ocean. Since the RAC is a surface current this energy is directly available for the melting of ice (icebergs, melange, and sea ice). While the melting of melange and icebergs merely reduces the temperature and freshen the surface water, changing the gas solubility, melting sea ice can release ikaite ($CaCO_3 \cdot 6H_2O$) which facilitates additional CO_2 gas dissolution (Rysgaard et al., 2009). Reduced sea ice cover is thought to facilitate primary productivity through enhanced availability of light, providing nutrients are also available (Bates et al., 2009) and rates of net primary productivity are thought to be increasing (Arrigo and van Dijken, 2015) even in the face of increasing stratification and the associated nutrient limitation (von Appen et al., 2021). The Arctic Ocean surface waters are nutrient limited (Tuerena et al., 2022) and the regions of extreme nitrate limitation are expanding, though primarily in the Western Arctic (Zhuang et al., 2021, 2022). As a result of surface water nutrient limitation primary producers are generally found under sea ice (Ardyna et al., 2020), in the sea ice marginal zone, particular where there is upwelling (Mundy et al., 2009), or as a 'deep chlorophyll maximum' (DCM) below the nitrogen depleted surface layer (Martin et al. (2013) and references therein). Since the DCM is not directly in contact with the atmosphere the uptake by primary producers is not directly associated with drawdown from the atmosphere unless the strong stratification is broken and has a chance to equilibrate prior to sea ice freeze up. This equilibration needs to occur before the produced organic carbon is remineralised and before sea ice cover is extensive enough to form a barrier between ocean and atmosphere. This dominance of DCM may be a recent development. During the 1990s, primary productivity on the northern Northeast Greenland shelf was found near the surface in the Northeast Water Polynya and the required nutrients were associated with water from beneath the landfast and glacial ice (Wallace et al., 1995a). This led to the development of the 'seasonal rectification hypothesis' which describes strong uptake of atmospheric CO_2 during the sea ice melt season by primary producers followed by a season of inhibited autumn CO_2 release to the atmosphere by the development of an extensive sea ice cover (Yager et al., 1995). Since then, the open water fraction in the region has changed dramatically as has the temperature of the Arctic river influenced Polar Water layer (De Steur et al., 2023). In the summer of 2017 the Northeast Greenland shelf experienced a sudden drop in sea ice cover starting in August 2017 initiating a previously unseen decline in Arctic Ocean sea ice export which persisted throughout 2018 (Sumata et al., 2022). These ice-free conditions allowed unprecedented access to previously unstudied parts of the Northeast Greenland shelf (Figure 1 a). The observations for this study were made opportunistically in these suddenly ice-free waters and may offer some insight into the response of the CO_2 system on the Northeast Greenland shelf to an increasingly warm and ice-free Arctic.

2 Materials & methods

2.1 Cruise & hydrographical setting

Data for this study was collected during two cruises (DANA2017 and NEGREEN2017). The hydrography of the Northeast Greenland shelf during these cruises was described in our previous paper (Willcox et al., 2023). To summarize briefly, several water types were found to be superimposed on much of the shelf albeit in different ways in different geographical areas. The hydrography is dominated by freshwater from various Arctic Ocean sources with different total alkalinity (Figure 1a) down to the depths of the Eurasian Basin Atlantic Water (EBAW) and Return Atlantic Water (RAW) which have similar practical salinities of respectively 34.8 and 35. The freshwater is primarily sourced from the Russian Shelf (particularly the Laptev Sea)

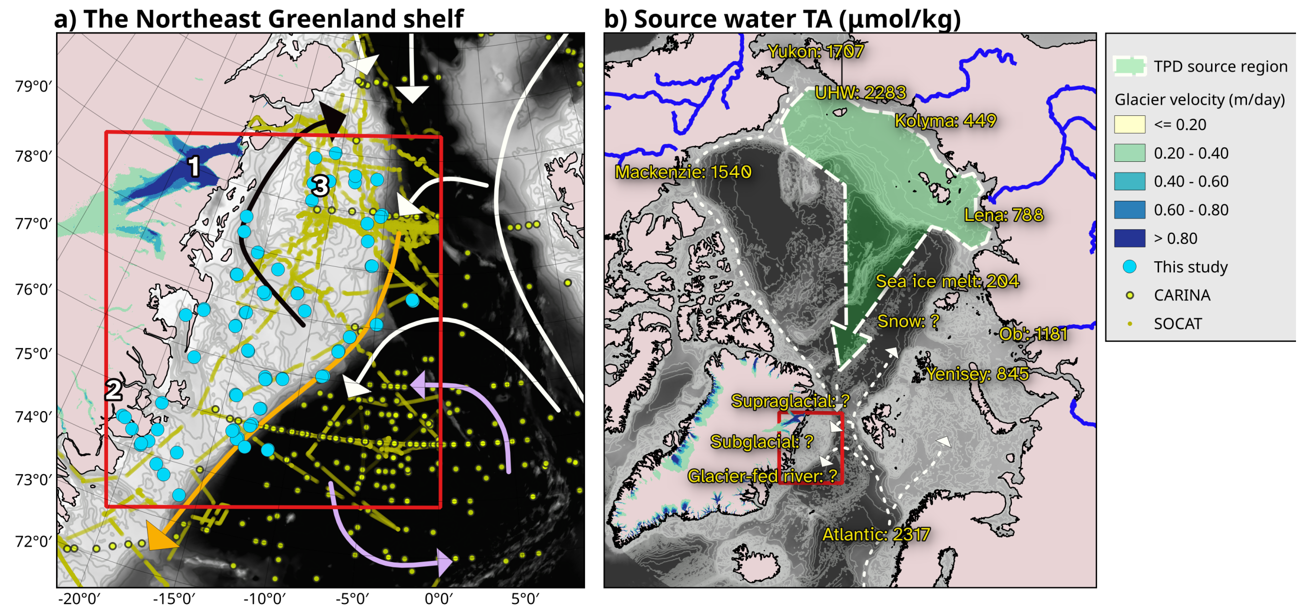

Figure 1. (a) Overview of carbon system chemistry and CO_2 fugacity (fCO_2) samples on the Northeast Greenland shelf. Arrows indicate known major currents. White indicates the advection of Arctic and Atlantic water, including Return Atlantic Water (RAW), Polar Surface Water (PSW), and Eurasian Basin or Arctic Atlantic Water (EBAW/AAW). Black is the Northeast Greenland Counter current (NEGCC) which transports water west then northward in a counterclockwise direction directly past the coast, purple is the Greenland Gyre, and orange is the East Greenland Current (EGC) which roughly follows the continental slope. SOCAT surface water fCO_2 measurement coordinates from Bakker et al. (2023), CARINA full depth carbon chemistry stations from Olsen (2009). Numbers 1, 2, and 3 refer to the Northeast Greenland Ice Stream (culminating in 79N glacier or Nioghalvfjerdsbrae and Zachariae Isstrom), Young Sund, and the Northeast Water Polynya region respectively. (b) Known sources of total alkalinity to the Arctic Ocean highlighting the source regions of the Transpolar drift (green area with dashed white outline) and the location of the study area (red rectangle). Sources to the Arctic Ocean include Arctic rivers with variable catchment geology, sea ice and snow melt, and the Pacific Water coming in through the Bering Strait. River TA values from Cooper et al. (2008), Pacific from Anderson et al. (2013), and Atlantic from Jones et al. (2021). Sea ice TA is from own measurements during these cruises Willcox et al. (2023). Locally, there is an unknown contribution of both sub- and supraglacial sources as well as glacier-fed rivers. Bathymetry was sourced from IBCAO (Jakobsson et al., 2020), sea ice extent from OSTIA (Good et al., 2020), and ice velocity from QGreenland v2 (Moon et al., 2022)

where vast amounts of riverine freshwater are introduced changing the salinity and surface water geochemical properties. This water is further geochemically modified in the Siberian shelf seas prior to cross-Arctic transport as a result of shallow bathymetry combined with high winds and extensive polynyas adding a measurable denitrification signal (Nitishinsky et al., 2007; Chang and Devol, 2009; Anderson et al., 2013) and changing the isotopic fractionation (Bauch et al., 2010). Finally the surface water masses are advected off of the Siberian continental shelves and entrained into the Transpolar Drift (TPD). Once entrained into the TPD the annual sea ice freeze-melt cycle will continue to freshen the surface layer by the export of brine and dilution with meltwater. This process diverts the slope of the surface water from that between Atlantic Water and meteoric freshwater toward the sea ice melt end-member in both TA-S and δ^{18}O-S diagrams. A comparison between the Laptev Sea and Northeast Greenland shelf in terms of apparent oxygen utilisation (AOU) against the nutrients phosphate and silicate, and nitrate to phosphate ratio, confirm the strong link between the Laptev Sea and the Northeast Greenland Shelf via the TPD. The surface water, located above the maximum Brunt-Väisälä frequency squared (N^2), and above the remnant of the winter mixed layer, is almost entirely depleted in nitrogen (median NO_3^- = 0 μmol/kg). Directly below this is a remnant of the winter mixed layer which exists at freezing temperatures and a practical salinity of ~ 31.4 psu (σ_T ~ 25). This is fresher than this inflection point was in previous decades (Budéus and Schneider, 1995; Budéus et al., 1997; Bignami and Hopkins, 1997). This layer contains, and apparently traps, the oxygen maximum indicating that it is not actively ventilated during the time when sampling occurred. From the salinity at the inflection point (and the oxygen maximum), there is a cold halocline layer which follows the freezing line up to a salinity of 34.0, the Lower Halocline Water. At this point we find another inflection away from the freezing line with a sharp temperature increase in temeprature to EBAW at 4 °C (S = 34.8) and AW at 6 °C (S = 35). The saltiest and warmest Atlantic Water found is likely sourced from the West-Spitsbergen Current. This water can be found at the surface just off the continental shelf and can make incursions onto the continental shelf, particularly further south. Surface conditions in terms of sea ice cover and surface temperature during the three weeks of the two cruises were variable (Figure 2) with warm surface temperatures and patchy sea ice dominating the first part, after which the sea ice fraction increased, particularly toward the north and north-west part of the shelf.

2.2 Sample Analysis

Descriptions for the analysis of the Conductivity, Temperature, and Depth (CTD) instrument data, nutrients, and total alkalinity are included in the methods section of Willcox et al. (2023). To analyse DIC, seawater samples were transferred from the CTD Rosette to gas-tight vials (12 mL Exetainer, Labco High Wycombe,UK), poisoned with 12 µL solution of saturated $HgCl_2$, and stored in the dark at room temperature until analysis. DIC was measured on a DIC analyzer (Apollo SciTech, Newark, DE, USA) by acidification of a 0.75 mL subsample with 1 mL 10% H_3PO_4 (Sigma-Aldrich, Saint-Louis, MO, USA), and quantification of the released CO_2 with a nondispersive infrared CO_2 analyzer (LI-COR, LI-7000, Lincoln, NE, USA). Results were then converted from μmol L^{-1} to μmol kg^{-1} based on sample density, which was estimated from salinity and temperature. An accuracy of $\pm$ 2 μmol kg^{-1} was determined for DIC from routine analysis of certified reference material (A.G. Dickson, Scripps Institution of Oceanography, San Diego, CA, USA).

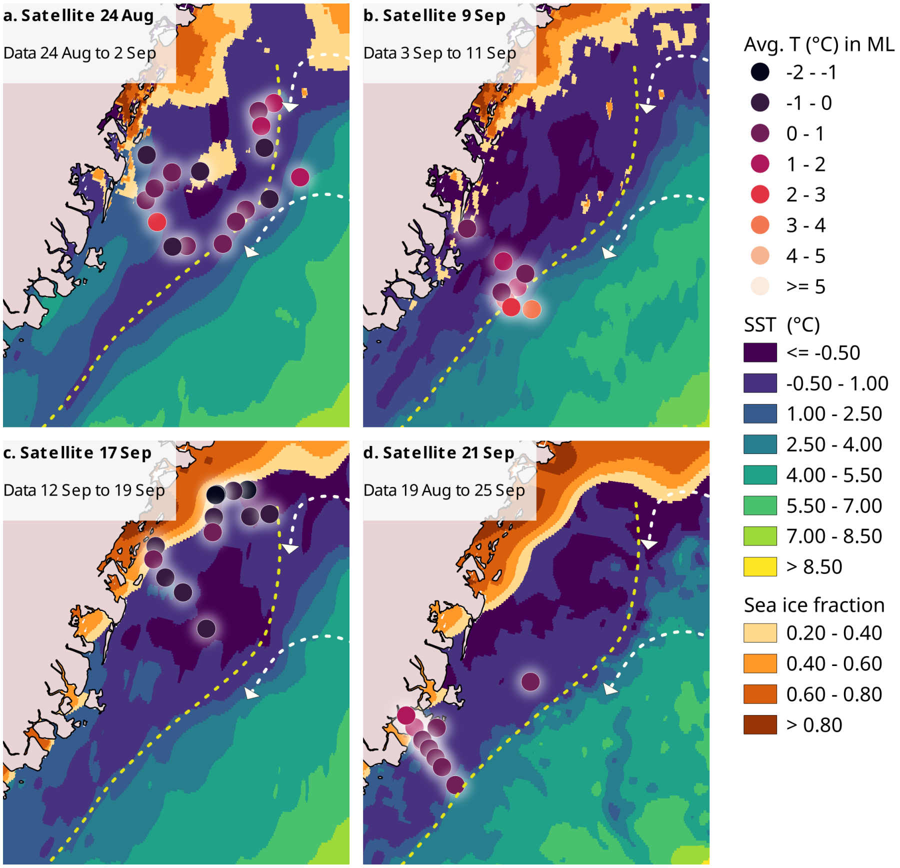

Figure 2. Surface conditions (sea ice fraction and sea surface temperature) on the shelf and average mixed layer depth temperature per station subdivided into four sampling periods. ESA sea surface temperature and sea ice fraction were obtained from Meteorological Office UK (2019) (Good et al., 2020). Average station mixed layer depth temperatures are the average temperature for all sampled depths above the maximum Brunt-Väisälä frequency squared (N^2)

CTD measurements of temperature and salinity were combined with the TA and DIC bottle data to calculate the pCO_2 using the program CO2SYS (van Heuven et al., 2011) with the dissociation constants k1 and k2 of Mehrbach et al. (1973) refitted by Dickson and Millero (1987) and the hydrogen sulfite dissociation constant from Dickson (1990).

2.3 Mixed layer depth determination

We estimate the depth of the mixed layer by determining that of the pycnocline through the determination of the maximum Brunt-Väisälä frequency (N^2) (Jones et al., 2021) for all stations with bottles taken shallower than 120 m depth. Our previous study indicated this would be a good proxy since the pycnocline acted as a barrier, trapping dissolved oxygen below it indicating that this water was not ventilated during the period of our study. The maximum N^2 was calculated for each CTD cast individually and depths varied between 1 and 30 m, with shallower depth closer to the coast and further north.

2.4 Normalisation of carbon chemistry bottle data

The bottle data were normalised by the application to the data of a fitted polynomial. The polynomial captures the effects of both the sea ice melt and meteopric freshwater dilution. A full justification, including a comparison with more traditional normalisation techniques, is provided in the Supplement with this manuscript.

2.5 Modified Z-score

Because the mean is heavily influenced by the extreme outliers in these data, parametric methods are not representative. Non-parametric methods relying on the median are more representative. The modified Z-score is one such method, it relies on the Mean Absolute Deviation (MAD). Data are marked as outliers when the modified Z-score is larger than a value D. Our choice of D (1.5) is discussed in the Supplement.

3 Results and discussion

Based on previous studies, the region is expected to act as a sink for atmospheric CO_2. Periods of high drawdown are specifically thought to occur when the light returns in spring allowing for autotrophic production during phytoplankton blooms including under ice blooms (Arrigo et al., 2012; Ardyna et al., 2020), and during upwelling events in the marginal ice zone (Mundy et al., 2009). The release of CO_2 during the dark season, when no photosynthesis can occur and the region becomes (net) heterotrophic, is inhibited by extensive sea ice cover (Yager et al., 1995). This ice-covered period can be associated with CO_2 supersaturation (Duke et al., 2021). Autumn is a transition period between a summer highly stratified environment where light is available and is dominated by sea ice and meteoric freshwater flux, and a winter environment that is dark, unproductive, and influenced by sea ice growth and brine rejection. In the northern North Atlantic, autumn is associated with the breakdown of stratification near the surface due to higher wind speeds and storms. This pattern is repeated in the Greenland Sea where average wind speeds tend to increase during the period of this study (days of year 240 - 256, Qu et al. (2012)), and August and September are associated with increasing concentrations of dissolved CO_2 after a seasonal low in July (Arrigo et al., 2010).

The fall of 2017 had exceptionally low sea ice cover for the region (Sumata et al., 2022), allowing unpecedented access to undersampled regions of the shelf. The parameters which usually explain most of the variability in carbon dioxide fugacity (fCO_2) in the ocean surface are temperature (T), salinity (S), total alkalinity (TA), and dissolved inorganic carbon (DIC). Gas solubility is expected to increase with decreasing temperature, change with salinity as a result of variable dissociation constants through their dependence on ion activities. With increasing TA, the fCO_2 is expected to decrease since these are the ions associated with increasing the ocean buffer capacity (Zeebe and Wolf-Gladrow, 2001), and DIC is taken up by autotrophs during primary production and converted to organic matter. The data collected on the Northeast Greenland shelf in fall of 2017 do not clearly show the patterns expected (Figure 3). The data are scattered and outliers do not follow a discernable pattern with respect to salinity or temperature. Outliers occur during both cruises, in measurements from both labs, toward high and low TA and DIC concentrations, and at different depths. There is no clear correlation between the outliers and any variable

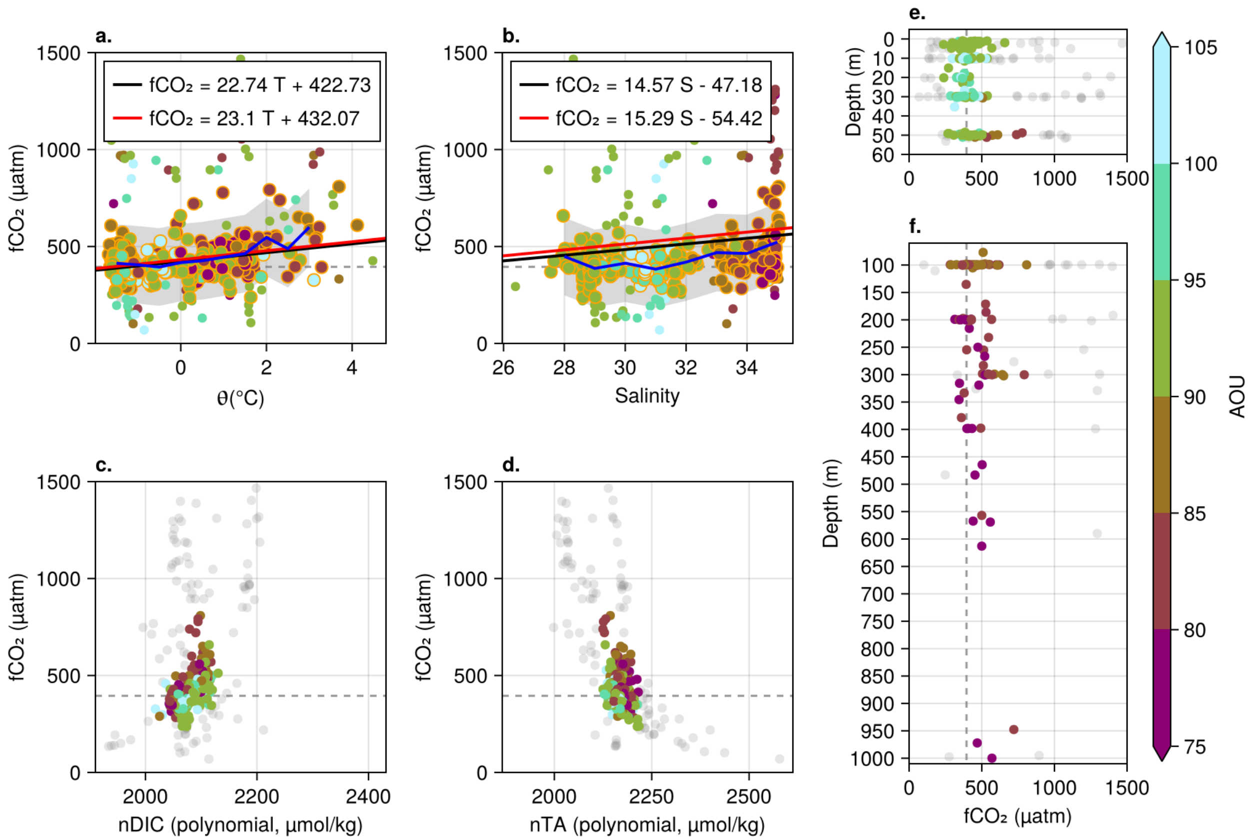

Figure 3. Carbon dioxide fugacity fCO_2 plotted as a function of potential temperature (a), practical salinity (b) normalised DIC (c), normalised TA (c), and with depth for shallower (e) and deeper waters (f). The orange lines in a,b are the best fit line for the median ± 200 fCO_2 for each step in controlling variable. The median for steps in salinity is shown as the blue line where values included in the median calculation (± 200) are bounded by the grey region. Data with orange stroke in a,b and in colour in c,d,e,f are values with a modified Z-score of within D ± 1.5. The red line in (a,b) is the modified Z-score data best fit

measured. We therefore have to surmise that at this time we are missing a (set of) variable(s) and/or process(es) with which to describe the extreme values in these data, and we do not have sufficient justification to remove any of the outliers from the dataset. We cannot discard any data without a good reason to flag it as an outlier, and with this amount of variability in the dataset using linear correlations loses some efficacy. Mean values are not representative of the data therefore any attempt at statistical analysis necessarily relies on non-parametric techniques such as the modified Z-score.

Using median values of fCO_2 for steps of each controlling variable (T, S, etc) rather than the mean and picking values for fCO_2 between which the correlation is to be made or using an extreme modified Z-score outlier flag (> D=1.5), a linear relationship can be established for temperature (Figure 3a). The same method fails for salinity (Figure 3b) because the median fCO_2 follows a slightly polynomial shape which means the line is an overestimate compared to the values calculated from

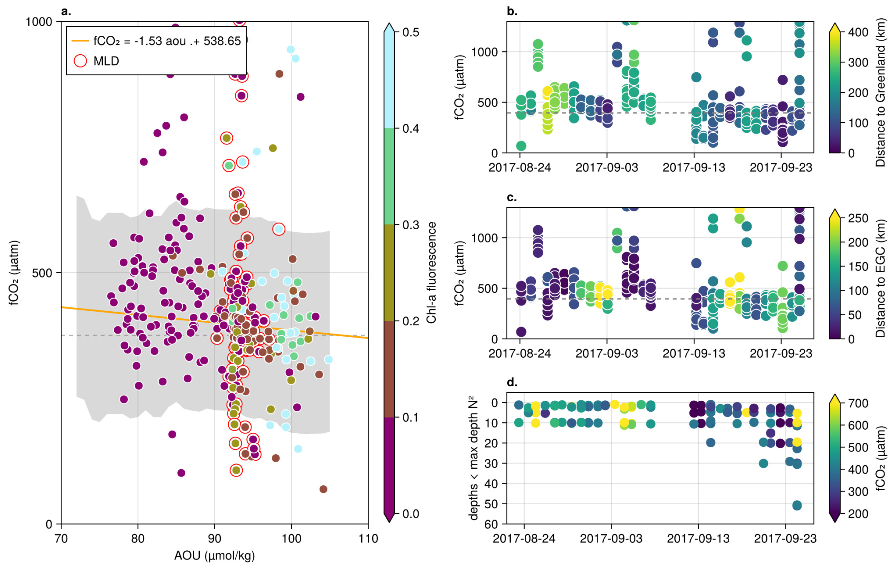

Figure 4. (a) the change in fCO_2 with changes in apparent oxygen utilisation (AOU). (b,c) fCO_2 changes with date, coloured respectively by distance of station to Greenland and the EGC (d) Data in the mixed layer depth (MLD) for each station by date

CO2SYS. The median and inter quartile range (iqr) for the mixed layer depth based on the N^2 are 410.49 and 147.58 μatm, which is above the projected atmospheric value for the region of 395 μatm based on SeaFlux (Fay et al., 2021) though this is for the entire time period which may not be representative (Figure 4). If we divide further by time, the period before 10 September has a median 477.66 with iqr 201.96 μatm and after this date the median goes down to 367.89 with iqr 110.66 μatm. This indicates a change in conditions, either between the sampling period or the sampling locations where the region turns from a source to a sink. For samples taken near the surface, the apparent oxygen utilisation is under 95% indicating either its use in biochemical processes, or the active ventilation of or mixing with waters with even lower dissolved oxygen concentrations. In case of the former, this may also be responsible for the some of the higher concentrations in surface layer fCO_2 though we have no additional evidence to show active remineralisation.

One of the reasons that the relationships between fCO_2 and temperature and salinity respectively is unpredictable and highly variable is that water types with different histories found on the Northeast Greenland shelf can have similar end-member values for certain parameters. For example, meteoric freshwater from the longer fjords has had time to heat up before being advected onto the shelf, with air temperatures in summer as high as 10 to 12 °C (Rysgaard et al., 2003). Atlantic Water (AW) from the return current also has temperatures of over 4 °C and a salinity of 35. Eurasian Basin Atlantic Water (EBAW) i.e. Arctic Atlantic Water that has circumnavigated the Eurasian Basin and lost heat is cold but has a salinity of 34.8. This is very close to AW salinity (34.8/35 = 0.99). The proportionality of the difference in TA between AW is similar to that in salinity, e.g. 0.98 for a EBAW TA of 2274 (Jones et al., 2008) and an AW TA of 2317 (Jones et al., 2021) but the 1% difference may be indicative of additional processes rendering TA non-conservative in this layer, diluted by a large volume. The region is also known for its small diameter (5 - 10 km) but deep penetrating eddies which offshelf can reach down to over 1000 m (Wadhams et al., 2002; Gascard et al., 2002; Rudels et al., 2005). With our sampling density which has distances between stations that are frequently over 30 km such features could create heterogeneous results for neighbouring station locations.

At depths below the surface mixed layer, as defined by the Brunt-Väisälä frequency squared (N^2), the AOU and fCO_2 are inversely correlated (Figure 3e). This ranges from the remnant of the winter mixed layer which is supersaturated with respect to dissolved oxygen, AOU > 100 %, and the median fCO_2 is lower than atmospheric values at 383.39 with an iqr of 130.40 μatm, to depths where AOU < 80 % and the fCO_2 has a median of 453.32 with an iqr of 119.61 μatm. The maximum AOU corresponds with higher Chloropyll *a* fluorescence in the remnant winter mixed layer which indicates that the dissolved bioactive gas concentrations in this layer are at least partially driven by the presence of a Deep Chlorophyll Maximum (DCM) (Figure 4a). While surface conditions were variable during the sampling period in terms of sea ice fraction and temperature (Figure 2), the region off-shelf, to the east of the EGC, is generally associated with warmer temperatures and higher salinity, while waters across the shelf itself have colder surface temperatures. Sea ice is most persistent in the north. The first part of the sampling period had warmer surface temperatures on the shelf itself, especially in the south along the coast. This is associated with higher fCO_2, particularly at higher distances from the Greenland coast and smaller distances to the slope (EGC). During the sampling period, the surface temperature cools and the sea ice in the north becomes more consolidated. The fCO_2 during the later period are much lower and trend below atmospheric saturation, potentially indicating a seasonal shift (Figure 4b,c). The increasing Mixed Layer Depth (MLD) near the end of the study (Figure 4d) could support this though this could also be attributable to another process such as the presence of a front.

The algorithms established by Arrigo et al. (2010) to determine TA and DIC for the North Atlantic (surface layer) fit our data well for TA, albeit with a lot of scatter (Figure 5 a). This is not entirely surprising since the dataset used for the algorithm was in part obtained from measurements of the northern part of the Northeast Greenland shelf (Wallace et al., 1995b). To determine the best fit for DIC, they removed values for nearshore waters proximal to riverine meteoric freshwater sources from the dataset due to those measurements being lower than the algorithmically predicted values. Our measurements are also lower than the values predicted using their algorithm even though they are not directly near a meteoric freshwater source (Figure 5 b). Similar linear regressions were fitted by Nondal et al. (2009) and Olsen (2009). The former do not provide an accurate reflection of our data and the second have a similar slope but a lower intercept. The Arrigo et al. (2010) equation is therefore the best predictor for TA on the shelf.

The difference between TA and DIC drives much of the fCO_2 variability calculated using CO2SYS, and increases (on average) between the first and second parts of the cruise (Figure 6a,b) as a result of a reduction in DIC. The average TA in the mixed layer remains the same throughout the study period. The reduction in mixed layer DIC relative to mixed layer TA is most pronounced at the lower latitudes in the southernmost transect near Young Sound (Figure 6 c).

As previously described in Henson et al. (2024), the depth-depedence of carbonate chemistry on the Northeast Greenland shelf is non-linear. Whether the surface mixed layer will act as a sink or a source of CO_2 with respect to the atmosphere seems to vary though it is clear that the region is not as strong a sink as previously expected and may be a net source. Increases in freshwater, both meteoric as well as sea ice melt, are associated with more corrosive surface waters near the coast in the region

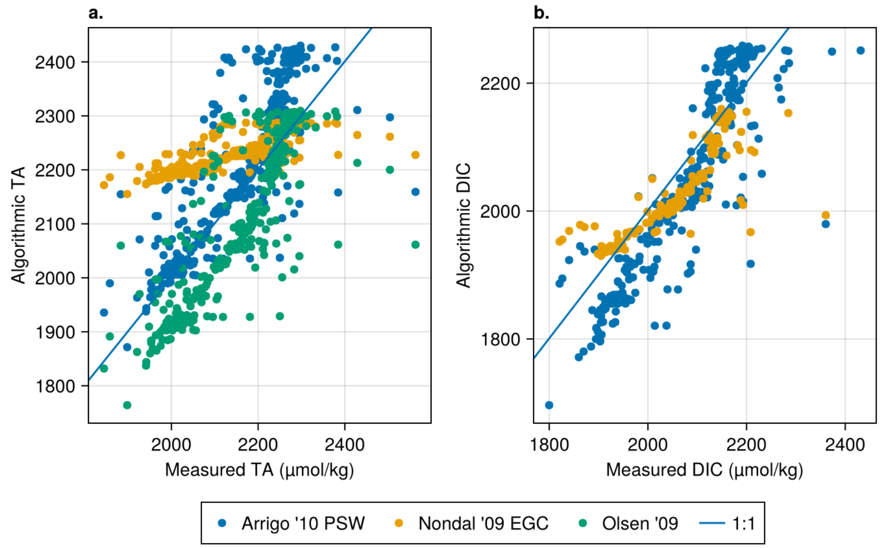

Figure 5. Measured concentrations of TA (a) and DIC (b) compared to values predicted using the algorithms from Arrigo et al. (2010), Nondal et al. (2009), and Olsen (2009). Since NO_3^- concentrations were only available for the last two weeks of the cruise, these are the only data shown for the Nondal et al. (2009) fit in (b)

(Henson et al., 2023) but this can be compensated for by high productivity stimulated by nutrient input from local ice melt (Wallace et al., 1995a; Fransson et al., 2023). If this is the case this may be another reason for the extreme variability of results we obtained. The mixed layer at the surface on the Northeast Greenland shelf that is advected in from the Arctic Ocean is already severely nitrogen depleted (Tuerena et al., 2022) which impacts opportunities for local primary producers to exist at the surface away from areas where local features such as eddies or actively melting sea ice might contribute nutrients to the surface water. Where sea ice melting, glacier melting, or potentially even iceberg fertilisation contribute nutrients to the surface, primary productivity can be quickly stimulated and the associated removal of DIC would allow for increased buffering by the TA and result in a lower fCO_2 in these areas. Sea ice and iceberg melt can be patchy and major continental meteoric freshwater contributions directly onto the shelf happen primarily at the termini of the 79N glacier and Zachariaea Isstrom, therefore the extent of surface primary productivity influencing the carbon system is likely limited during the sampling period. The rest of the shelf receives local freshwater input from long fjords where all the nutrients added in the surface have likely already been fully utilised before they reach the shelf (Holding et al., 2019). This means that primary productivity is necessarily limited to a deep chlorophyll maximum (DCM) below the nitracline. During years of more extensive sea ice cover primary production may occur closer to the surface and stimulate more direct uptake of CO_2 from the atmosphere. Higher benthic productivity has been observed closer to the EGC which, with strong benthic-pelagic coupling in the region, indicates higher productivity at the surface near the slope (Bodur et al., 2024) and an associated higher uptake of CO_2. In the absence of sea ice melt it is possible

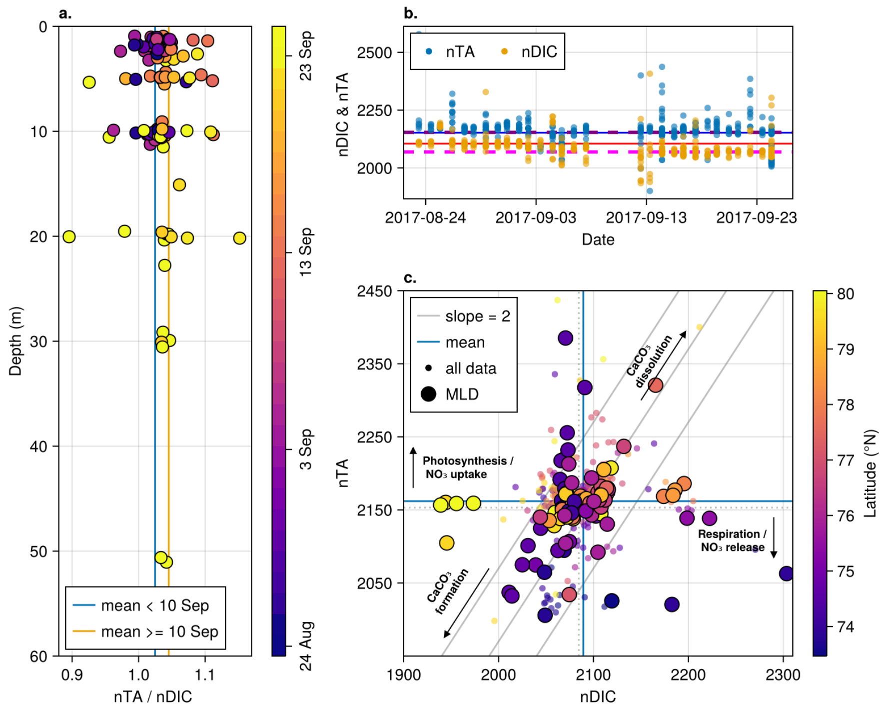

Figure 6. (a) Mixed layer nTA/nDIC with depth for the surface mixed layer. (b) nTA and nDIC respectively by measurement date. Blue line is TA and orange line DIC best fit between 24 Aug - 10 Sep. Dashed lines are for dates after 10 Sep. (c) nTA against nDIC

that this is stimulated by along-shelf upwelling or by EGC-associated eddies which are particularly prominent in areas where the density of the warm Atlantic and the cool Polar Water are the same (Bashmachnikov et al., 2020).

4 Summary

We present the first full depth carbon system observations of the area of the Northeast Greenland shelf between 75 and 79 °N, with additional measurements outside of Young Sund and in the region of the Northeast Water Polynya. Our total alkalinity (TA) measurements correspond well to the predictive algorithm created by Arrigo et al. (2010), whereas the dissolved inorganic carbon (DIC) measurements are lower than predicted by these authors. We find that the shelf does not act as a consistent sink as expected per the calculated fugacity of carbon dioxide (fCO_2) from samples of TA and DIC. Using non-parametric methods due to the large number of outliers in the dataset, we find that the surface of the region can act as either a sink or source of CO_2 with respect to the atmosphere. The highest uptake is associated with a maximum in apparent oxygen utilisation (AOU) and chlorophyll within the remnant of the winter mixed layer where there is both light and nutrient availability. This water is not actively ventilated and therefore cannot contribute directly to atmospheric carbon exchange. The middle of the study period saw an apparent breakdown in stratification based on an increase in mixed layer depth as determined by the maximum

Brunt-Väisälä frequency squared (N^2). This was associated with a reduction in surface layer fCO_2 to median values below the expected atmospheric concentration, apparently due to a corresponding reduction in DIC. The many outliers in fCO_2, particularly in the surface mixed layer, are not clearly associated with any known process or measured variable. It is likely that the shelf is characterised by influences at smaller scales than the sampling density of this study. August and September 2017 were extraordinary in terms of low sea ice cover, which was the reason that opportunistic sampling of this previously unsampled area could take place. Our results may therefore not represent a baseline for the region when ice covered but rather may act as an example of the response of the region to future increases in oceanic and atmospheric heat and reductions in sea ice.

Data availability. We are currently involved in adding the data to the Pangaea data repository and will make the set available as soon as they have accepted it

Author contributions. The fieldwork component including taking samples from the CTD was performed by Thomas Juul-Pedersen, Johnna Michelle Holding, and Søren Rysgaard Marcos Lemes and Mikael Sejr performed the geochemical laboratory measurements for TA and DIC in their institutes respectively. Subsequent data analysis, writing of code, and initial drafting of the manuscript was performed by the primary author. Extensive feedback on first and second drafts of the manuscript was obtained from all co-authors.

Competing interests. The authors declare no competing interests.

Acknowledgements. We would like to thank our manuscript reviewers for providing detailed and relevant feedback and making a positive contribution to this manuscript. The cruises were funded through the Greenland Ecosystem Monitoring Program (Leg 1), the Danish Centre for Marine Research, the Natural Sciences and Engineering Research Council of Canada (NSERC), and the Independent Research Fund Denmark (G-Ice Project) (Grant 7014-00113B/FNU) (Leg 2). This study received financial support from the Aage V Jensens Foundation, the Arctic Research Centre, Aarhus University, and Independent Research Fund Denmark (GreenShelf project (Grant 0135-00165B/FNU) to MSS). The captain and crew of RV DANA are acknowledged for excellent assistance during our field cruise to NE Greenland. Egon Frandsen is acknowledged for support on logistics and operations.

References

Anderson, L. G., Andersson, P. S., Björk, G., Peter Jones, E., Jutterström, S., and Wåhlström, I.: Source and formation of the upper halocline of the Arctic Ocean, Journal of Geophysical Research: Oceans, 118, 410–421, https://doi.org/10.1029/2012JC008291, 2013.

Ardyna, M., Mundy, C. J., Mayot, N., Matthes, L. C., Oziel, L., Horvat, C., Leu, E., Assmy, P., Hill, V., Matrai, P. A., Gale, M., Melnikov, I. A., and Arrigo, K. R.: Under-Ice Phytoplankton Blooms: Shedding Light on the "Invisible" Part of Arctic Primary Production, Frontiers in Marine Science, 7, 608 032, https://doi.org/10.3389/fmars.2020.608032, 2020.

Arrigo, K. R. and van Dijken, G. L.: Continued increases in Arctic Ocean primary production, Progress in Oceanography, 136, 60–70, https://doi.org/10/f7mdc6, 2015.

Arrigo, K. R., Pabi, S., van Dijken, G. L., and Maslowski, W.: Air-sea flux of CO2 in the Arctic Ocean, 1998–2003, Journal of Geophysical Research, 115, G04 024, https://doi.org/10.1029/2009jg001224, 2010.

Arrigo, K. R., Perovich, D. K., Pickart, R. S., Brown, Z. W., Van Dijken, G. L., Lowry, K. E., Mills, M. M., Palmer, M. A., Balch, W. M., Bahr, F., Bates, N. R., Benitez-Nelson, C., Bowler, B., Brownlee, E., Ehn, J. K., Frey, K. E., Garley, R., Laney, S. R., Lubelczyk, L., Mathis, J., Matsuoka, A., Mitchell, B. G., Moore, G. W. K., Ortega-Retuerta, E., Pal, S., Polashenski, C. M., Reynolds, R. A., Schieber, B., Sosik, H. M., Stephens, M., and Swift, J. H.: Massive Phytoplankton Blooms Under Arctic Sea Ice, Science, 336, 1408–1408, https://doi.org/10.1126/science.1215065, 2012.

Bakker, D. C. E., Alin, S. R., Bates, N., Becker, M., Feely, R. A., Gkritzalis, T., Jones, S. D., Kozyr, A., Lauvset, S. K., Metzl, N., Munro, D. R., Nakaoka, S.-I., Nojiri, Y., O'Brien, K. M., Olsen, A., Pierrot, D., Rehder, G., Steinhoff, T., Sutton, A. J., Sweeney, C., Tilbrook, B., Wada, C., Wanninkhof, R., Akl, J., Barbero, L., Beatty, C. M., Berghoff, C. F., Bittig, H. C., Bott, R., Burger, E. F., Cai, W.-J., Castaño-Primo, R., Corredor, J. E., Cronin, M., De Carlo, E. H., DeGrandpre, M. D., Dietrich, C., Drennan, W. M., Emerson, S. R., Enochs, I. C., Enyo, K., Epherra, L., Evans, W., Fiedler, B., Fontela, M., Frangoulis, C., Gehrung, M., Giannoudi, L., Glockzin, M., Hales, B., Howden, S. D., Ibánhez, J. S. P., Kamb, L., Körtzinger, A., Lefèvre, N., Lo Monaco, C., Lutz, V. A., Macovei, V. A., Maenner Jones, S., Manalang, D., Manzello, D. P., Metzl, N., Mickett, J., Millero, F. J., Monacci, N. M., Morell, J. M., Musielewicz, S., Neill, C., Newberger, T., Newton, J., Noakes, S., Ólafsdóttir, S. R., Ono, T., Osborne, J., Padín, X. A., Paulsen, M., Perivoliotis, L., Petersen, W., Petihakis, G., Plueddemann, A. J., Rodriguez, C., Rutgersson, A., Sabine, C. L., Salisbury, J. E., Schlitzer, R., Skjelvan, I., Stamataki, N., Sullivan, K. F., Sutherland, S. C., T'Jampens, M., Tadokoro, K., Tanhua, T., Telszewski, M., Theetaert, H., Tomlinson, M., Vandemark, D., Velo, A., Voynova, Y. G., Weller, R. A., Whitehead, C., and Wimart-Rousseau, C.: Surface Ocean CO2 Atlas Database Version 2023 (SOCATv2023) (NCEI Accession 0278913), https://doi.org/10.25921/R7XA-BT92, 2023.

Bashmachnikov, I. L., Kozlov, I. E., Petrenko, L. A., Glok, N. I., and Wekerle, C.: Eddies in the North Greenland Sea and Fram Strait From Satellite Altimetry, SAR and High-Resolution Model Data, Journal of Geophysical Research: Oceans, 125, e2019JC015 832, https://doi.org/10.1029/2019JC015832, 2020.

Bates, N. R., Mathis, J. T., and Cooper, L. W.: Ocean acidification and biologically induced seasonality of carbonate mineral saturation states in the western Arctic Ocean, Journal of Geophysical Research, 114, C11 007, https://doi.org/10.1029/2008jc004862, 2009.

Bauch, D., Hölemann, J., Willmes, S., Gröger, M., Novikhin, A., Nikulina, A., Kassens, H., and Timokhov, L.: Changes in distribution of brine waters on the Laptev Sea shelf in 2007, Journal of Geophysical Research, 115, C11 008, https://doi.org/10.1029/2010JC006249, 2010.

Bignami, F. and Hopkins, T.: The water mass characteristics of the Northeast Water Polynya: Polar Sea data 1992–1993, Journal of Marine Systems, 10, 139–156, https://doi.org/10.1016/S0924-7963(96)00079-6, 1997.

Bodur, Y. V., Renaud, P. E., Lins, L., Da Costa Monteiro, L., Ambrose, W. G., Felden, J., Krumpen, T., Wenzhöfer, F., Włodarska-Kowalczuk, M., and Braeckman, U.: Weakened pelagic-benthic coupling on an Arctic outflow shelf (Northeast Greenland) suggested by benthic ecosystem changes, Elem Sci Anth, 12, 00 005, https://doi.org/10.1525/elementa.2023.00005, 2024.

Broecker, W. S.: Thermohaline Circulation, the Achilles Heel of Our Climate System: Will Man-Made CO_2 Upset the Current Balance?, Science, 278, 1582–1588, https://doi.org/10.1126/science.278.5343.1582, 1997.

Budéus, G. and Schneider, W.: On the hydrography of the Northeast Water Polynya, Journal of Geophysical Research, 100, 4287, https://doi.org/10.1029/94jc02024, 1995.

Budéus, G., Schneider, W., and Kattner, G.: Distribution and exchange of water masses in the Northeast Water polynya (Greenland Sea), Journal of Marine Systems, 10, 123–138, https://doi.org/10.1016/s0924-7963(96)00074-7, 1997.

Carmack, E. and Wassmann, P.: Food webs and physical–biological coupling on pan-Arctic shelves: Unifying concepts and comprehensive perspectives, Progress in Oceanography, 71, 446–477, https://doi.org/10.1016/j.pocean.2006.10.004, 2006.

Chang, B. X. and Devol, A. H.: Seasonal and spatial patterns of sedimentary denitrification rates in the Chukchi sea, Deep Sea Research Part II: Topical Studies in Oceanography, 56, 1339–1350, https://doi.org/10.1016/j.dsr2.2008.10.024, 2009.

Cooper, L. W., McClelland, J. W., Holmes, R. M., Raymond, P. A., Gibson, J. J., Guay, C. K., and Peterson, B. J.: Flow-weighted values of runoff tracers (d18O, DOC, Ba, alkalinity) from the six largest Arctic rivers, Geophysical Research Letters, 35, L18 606, https://doi.org/10.1029/2008gl035007, 2008.

De Steur, L., Sumata, H., Divine, D. V., Granskog, M. A., and Pavlova, O.: Upper ocean warming and sea ice reduction in the East Greenland Current from 2003 to 2019, Communications Earth & Environment, 4, 261, https://doi.org/10.1038/s43247-023-00913-3, 2023.

Dickson, A. and Millero, F.: A comparison of the equilibrium constants for the dissociation of carbonic acid in seawater media, Deep Sea Research Part A. Oceanographic Research Papers, 34, 1733–1743, https://doi.org/10.1016/0198-0149(87)90021-5, 1987.

Dickson, A. G.: Standard potential of the reaction: AgCl(s) +iH,(g) = Ag(s) + HCl(aq), and and the standard acidity constant of the ion HSOh in synthetic sea water from 273.15 to 318.15 K, Journal of Chemical Thermodynamics, 22, 113–127, https://doi.org/10.1016/0021-9614(90)90074-Z, 1990.

Duke, P. J., Else, B. G. T., Jones, S. F., Marriot, S., Ahmed, M. M. M., Nandan, V., Butterworth, B., Gonski, S. F., Dewey, R., Sastri, A., Miller, L. A., Simpson, K. G., and Thomas, H.: Seasonal marine carbon system processes in an Arctic coastal landfast sea ice environment observed with an innovative underwater sensor platform, Elementa: Science of the Anthropocene, 9, 00 103, https://doi.org/10.1525/elementa.2021.00103, 2021.

Ericson, Y., Fransson, A., Chierici, M., Jones, E. M., Skjelvan, I., Omar, A., Olsen, A., and Becker, M.: Rapid fCO2 rise in the northern Barents Sea and Nansen Basin, Progress in Oceanography, 217, 103 079, https://doi.org/10.1016/j.pocean.2023.103079, 2023.

Farmer, J. R., Hönisch, B., Haynes, L. L., Kroon, D., Jung, S., Ford, H. L., Raymo, M. E., Jaume-Seguí, M., Bell, D. B., Goldstein, S. L., Pena, L. D., Yehudai, M., and Kim, J.: Deep Atlantic Ocean carbon storage and the rise of 100,000-year glacial cycles, Nature Geoscience, 12, 355–360, https://doi.org/10.1038/s41561-019-0334-6, 2019.

Fay, A. R., Gregor, L., Landschützer, P., McKinley, G. A., Gruber, N., Gehlen, M., Iida, Y., Laruelle, G. G., Rödenbeck, C., Roobaert, A., and Zeng, J.: SeaFlux: harmonization of air–sea CO2 fluxes from surface pCO2 data products using a standardized approach, Earth System Science Data, 13, 4693–4710, https://doi.org/10.5194/essd-13-4693-2021, 2021.

Fransson, A., Chierici, M., Granskog, M. A., Dodd, P. A., and Stedmon, C. A.: Impacts of glacial and sea-ice meltwater, primary production, and ocean CO2 uptake on ocean acidification state of waters by the 79 North Glacier and northeast Greenland shelf, Frontiers in Marine Science, 10, 1155 126, https://doi.org/10.3389/fmars.2023.1155126, 2023.

Gascard, J.-C., Watson, A. J., Messias, M.-J., Olsson, K. A., Johannessen, T., and Simonsen, K.: Long-lived vortices as a mode of deep ventilation in the Greenland Sea, Nature, 416, 525–527, https://doi.org/10.1038/416525a, 2002.

Good, S., Fiedler, E., Mao, C., Martin, M. J., Maycock, A., Reid, R., Roberts-Jones, J., Searle, T., Waters, J., While, J., and Worsfold, M.: The Current Configuration of the OSTIA System for Operational Production of Foundation Sea Surface Temperature and Ice Concentration Analyses, Remote Sensing, 12, 720, https://doi.org/10.3390/rs12040720, 2020.

Henson, H. C., Holding, J. M., Meire, L., Rysgaard, S., Stedmon, C. A., Stuart-Lee, A., Bendtsen, J., and Sejr, M.: Coastal freshening drives acidification state in Greenland fjords, Science of The Total Environment, 855, 158 962, https://doi.org/10.1016/j.scitotenv.2022.158962, 2023.

Henson, H. C., Sejr, M. K., Meire, L., Sørensen, L. L., Winding, M. H., and Holding, J. M.: Resolving heterogeneity in CO2 uptake potential in the Greenland coastal ocean, https://doi.org/10.22541/essoar.171052503.36306724/v1, 2024.

Holding, J. M., Markager, S., Juul-Pedersen, T., Paulsen, M. L., Møller, E. F., Meire, L., and Sejr, M. K.: Seasonal and spatial patterns of primary production in a high-latitude fjord affected by Greenland Ice Sheet run-off, Biogeosciences, 16, 3777–3792, https://doi.org/10.5194/bg-16-3777-2019, 2019.

Hunt, G. L., Drinkwater, K. F., Arrigo, K., Berge, J., Daly, K. L., Danielson, S., Daase, M., Hop, H., Isla, E., Karnovsky, N., Laidre, K., Mueter, F. J., Murphy, E. J., Renaud, P. E., Smith, W. O., Trathan, P., Turner, J., and Wolf-Gladrow, D.: Advection in polar and sub-polar environments: Impacts on high latitude marine ecosystems, Progress in Oceanography, 149, 40–81, https://doi.org/10.1016/j.pocean.2016.10.004, 2016.

Jakobsson, M., Mayer, L. A., Bringensparr, C., Castro, C. F., Mohammad, R., Johnson, P., Ketter, T., Accettella, D., Amblas, D., An, L., Arndt, J. E., Canals, M., Casamor, J. L., Chauché, N., Coakley, B., Danielson, S., Demarte, M., Dickson, M.-L., Dorschel, B., Dowdeswell, J. A., Dreutter, S., Fremand, A. C., Gallant, D., Hall, J. K., Hehemann, L., Hodnesdal, H., Hong, J., Ivaldi, R., Kane, E., Klaucke, I., Krawczyk, D. W., Kristoffersen, Y., Kuipers, B. R., Millan, R., Masetti, G., Morlighem, M., Noormets, R., Prescott, M. M., Rebesco, M., Rignot, E., Semiletov, I., Tate, A. J., Travaglini, P., Velicogna, I., Weatherall, P., Weinrebe, W., Willis, J. K., Wood, M., Zarayskaya, Y., Zhang, T., Zimmermann, M., and Zinglersen, K. B.: The International Bathymetric Chart of the Arctic Ocean Version 4.0, Scientific Data, 7, 176, https://doi.org/10.1038/s41597-020-0520-9, 2020.

Jones, E., Anderson, L., Jutterström, S., and Swift, J.: Sources and distribution of fresh water in the East Greenland Current, Progress in Oceanography, 78, 37–44, https://doi.org/10.1016/j.pocean.2007.06.003, 2008.

Jones, E. M., Chierici, M., Menze, S., Fransson, A., Ingvaldsen, R. B., and Lødemel, H. H.: Ocean acidification state variability of the Atlantic Arctic Ocean around northern Svalbard, Progress in Oceanography, 199, 102 708, https://doi.org/10.1016/j.pocean.2021.102708, 2021.

Martin, J., Dumont, D., and Tremblay, J.-É.: Contribution of subsurface chlorophyll maxima to primary production in the coastal Beaufort Sea (Canadian Arctic): A model assessment: CONTRIBUTION OF SCM IN BEAUFORT SEA, Journal of Geophysical Research: Oceans, 118, 5873–5886, https://doi.org/10.1002/2013JC008843, 2013.

Mehrbach, C., Culberson, C. H., Hawley, J. E., and Pytkowicx, R. M.: Measurement of the apparent dissociation constants of carbonic acid in seawater at atmospheric pressure, Limnology and Oceanography, 18, 897–907, https://doi.org/10.4319/lo.1973.18.6.0897, 1973.

Meteorological Office UK: ESA SST CCI and C3S reprocessed sea surface temperature analyses, https://doi.org/10.48670/MOI-00169, 2019.

Michel, C., Hamilton, J., Hansen, E., Barber, D., Reigstad, M., Iacozza, J., Seuthe, L., and Niemi, A.: Arctic Ocean outflow shelves in the changing Arctic: A review and perspectives, Progress in Oceanography, 139, 66–88, https://doi.org/10.1016/j.pocean.2015.08.007, tex.ids= michel_arctic_2015-1, michel_arctic_2015-2, 2015.

Moon, T. A., Fisher, M., Harden, L., Shimonoko, H., and Stafford, T.: QGreenland (v2.0.0), https://qgreenland.org, https://doi.org/10.5281/zenodo.6369184, 2022.

Mundy, C. J., Gosselin, M., Ehn, J., Gratton, Y., Rossnagel, A., Barber, D. G., Martin, J., Tremblay, J.-É., Palmer, M., Arrigo, K. R., Darnis, G., Fortier, L., Else, B., and Papakyriakou, T.: Contribution of under-ice primary production to an ice-edge upwelling phytoplankton bloom in the Canadian Beaufort Sea, Geophysical Research Letters, 36, 2009GL038 837, https://doi.org/10.1029/2009GL038837, 2009.

Nakaoka, S.-I., Aoki, S., Nakazawa, T., Hashida, G., Morimoto, S., Yamanouchi, T., and Yoshikawa-Inoue, H.: Temporal and spatial variations of oceanic pCO_2 and air–sea CO_2 flux in the Greenland Sea and the Barents Sea, Tellus B: Chemical and Physical Meteorology, 58, 148, https://doi.org/10.1111/j.1600-0889.2006.00178.x, 2006.

Nitishinsky, M., Anderson, L. G., and Hölemann, J. A.: Inorganic carbon and nutrient fluxes on the Arctic Shelf, Continental Shelf Research, 27, 1584–1599, https://doi.org/10.1016/j.csr.2007.01.019, 2007.

Nondal, G., Bellerby, R. G. J., Olsen, A., Johannessen, T., and Olafsson, J.: Optimal evaluation of the surface ocean CO2 system in the northern North Atlantic using data from voluntary observing ships, Limnology and Oceanography: Methods, 7, 109–118, https://doi.org/10.4319/lom.2009.7.109, _eprint: https://onlinelibrary.wiley.com/doi/pdf/10.4319/lom.2009.7.109, 2009.

Olafsson, J., Olafsdottir, S. R., Takahashi, T., Danielsen, M., and Arnarson, T. S.: Enhancement of the North Atlantic CO_2 sink by Arctic Waters, Biogeosciences, 18, 1689–1701, https://doi.org/10.5194/bg-18-1689-2021, 2021.

Olsen, A.: Nordic Seas total alkalinity data in CARINA, Earth System Science Data, 1, 77–86, https://doi.org/10.5194/essd-1-77-2009, 2009.

Olsen, A., Brown, K. R., Chierici, M., Johannessen, T., and Neill, C.: Sea-surface CO2 fugacity in the subpolar North Atlantic, Biogeosciences, 5, 535–547, https://doi.org/10.5194/bg-5-535-2008, 2008.

Overland, J., Dunlea, E., Box, J. E., Corell, R., Forsius, M., Kattsov, V., Olsen, M. S., Pawlak, J., Reiersen, L.-O., and Wang, M.: The urgency of Arctic change, Polar Science, 21, 6–13, https://doi.org/10.1016/j.polar.2018.11.008, 2019.

Polyakov, I. V., Pnyushkov, A. V., Alkire, M. B., Ashik, I. M., Baumann, T. M., Carmack, E. C., Goszczko, I., Guthrie, J., Ivanov, V. V., Kanzow, T., Krishfield, R., Kwok, R., Sundfjord, A., Morison, J., Rember, R., and Yulin, A.: Greater role for Atlantic inflows on sea-ice loss in the Eurasian Basin of the Arctic Ocean, Science, 356, 285–291, https://doi.org/10.1126/science.aai8204, 2017.

Polyakov, I. V., Rippeth, T. P., Fer, I., Alkire, M. B., Baumann, T. M., Carmack, E. C., Ingvaldsen, R., Ivanov, V. V., Janout, M., Lind, S., Padman, L., Pnyushkov, A. V., and Rember, R.: Weakening of Cold Halocline Layer Exposes Sea Ice to Oceanic Heat in the Eastern Arctic Ocean, Journal of Climate, 33, 8107–8123, https://doi.org/10.1175/JCLI-D-19-0976.1, 2020.

Qu, B., Gabric, A. J., Zhu, J.-n., Lin, D.-r., Qian, F., and Zhao, M.: Correlation between sea surface temperature and wind speed in Greenland Sea and their relationships with NAO variability, 5, 2012.

Rajasakaren, B., Jeansson, E., Olsen, A., Tanhua, T., Johannessen, T., and Smethie, W.: Trends in anthropogenic carbon in the Arctic Ocean, Progress in Oceanography, 178, 102 177, https://doi.org/10.1016/j.pocean.2019.102177, 2019.

Richter-Menge, J., Overland, J. E., Mathis, J. T., Osborne, E., Brown, R., Mudryk, L., Luojus, K., and Helfrich, S.: Arctic Report Card 2017, Tech. rep., 2017.

Rudels, B., Björk, G., Nilsson, J., Winsor, P., Lake, I., and Nohr, C.: The interaction between waters from the Arctic Ocean and the Nordic Seas north of Fram Strait and along the East Greenland Current: results from the Arctic Ocean-02 Oden expedition, Journal of Marine Systems, 55, 1–30, https://doi.org/10.1016/j.jmarsys.2004.06.008, 2005.

Rysgaard, S., Vang, T., Stjernholm, M., Rasmussen, B., Windelin, A., and Kiilsholm, S.: Physical Conditions, Carbon Transport, and Climate Change Impacts in a Northeast Greenland Fjord, Arctic, Antarctic, and Alpine Research, 35, 301–312, https://doi.org/10.1657/1523-0430(2003)035[0301:PCCTAC]2.0.CO;2, 2003.

Rysgaard, S., Bendtsen, J., Pedersen, L. T., Ramløv, H., and Glud, R. N.: Increased CO2 uptake due to sea ice growth and decay in the Nordic Seas, Journal of Geophysical Research, 114, C09 011, https://doi.org/10.1029/2008JC005088, tex.ids: rysgaard_increased_2009-1, rysgaard_increased_2009-2, 2009.

Sejr, M., Krause-Jensen, D., Rysgaard, S., Sørensen, L., Christensen, P., and Glud, R.: Air—sea flux of CO_2 in arctic coastal waters influenced by glacial melt water and sea ice, Tellus B: Chemical and Physical Meteorology, 63, 815–822, https://doi.org/10.1111/j.1600-0889.2011.00540.x, 2011.

Serreze, M. C. and Barry, R. G.: Processes and impacts of Arctic amplification: A research synthesis, Global and Planetary Change, 77, 85–96, https://doi.org/10.1016/j.gloplacha.2011.03.004, 2011.

Shiklomanov, A., Déry, S., Tretiakov, M., Yang, D., Magritsky, D., Georgiadi, A., and Tang, W.: River freshwater flux to the arctic ocean, in: Arctic hydrology, permafrost and ecosystems, edited by Yang, D. and Kane, D. L., pp. 703–738, Springer International Publishing, Cham, https://doi.org/10.1007/978-3-030-50930-9_24, 2021.

Smethie, J. W. M. and Fine, R. A.: Rates of North Atlantic Deep Water formation calculated from chlorofluorocarbon inventories, p. 27, 2001.

Stroh, J., Kirillov, S., Panteleev, G., Francis, O., Yaremchuk, M., Bloshkina, E., and Lebedev, N.: Changes in Arctic Ocean Climate Evinced through Analysis of IPY 2007–2008 Oceanographic Observations, in: Arctic Studies - A Proxy for Climate Change, edited by Kanao, M., Kakinami, Y., and Toyokuni, G., IntechOpen, https://doi.org/10.5772/intechopen.80926, 2019.

Sumata, H., De Steur, L., Gerland, S., Divine, D. V., and Pavlova, O.: Unprecedented decline of Arctic sea ice outflow in 2018, Nature Communications, 13, 1747, https://doi.org/10.1038/s41467-022-29470-7, 2022.

Takahashi, T., Sutherland, S., Chipman, D., Goddard, J., Ho, C., Newberger, T., Sweeney, C., and Munro, D.: Climatological distributions of pH, pCO2, total CO2, alkalinity, and CaCO3 saturation in the global surface ocean, and temporal changes at selected locations, Marine Chemistry, 164, 95–125, https://doi.org/10.1016/j.marchem.2014.06.004, tex.ids= takahashi_climatological_2014-1, 2014.

Tuerena, R. E., Mahaffey, C., Henley, S. F., De La Vega, C., Norman, L., Brand, T., Sanders, T., Debyser, M., Dähnke, K., Braun, J., and März, C.: Nutrient pathways and their susceptibility to past and future change in the Eurasian Arctic Ocean, Ambio, 51, 355–369, https://doi.org/10.1007/s13280-021-01673-0, 2022.

van Heuven, S., Pierrot, D., Rae, J., Lewis, E., and Wallace, D.: CO2SYS v 1.1, MATLAB program developed for CO2 system calculations, ORNL/CDIAC-105b. Carbon Dioxide Information Analysis Center, Oak Ridge National Laboratory, U.S. DoE, Oak Ridge, TN., 2011.

von Appen, W.-J., Waite, A. M., Bergmann, M., Bienhold, C., Boebel, O., Bracher, A., Cisewski, B., Hagemann, J., Hoppema, M., Iversen, M. H., Konrad, C., Krumpen, T., Lochthofen, N., Metfies, K., Niehoff, B., Nöthig, E.-M., Purser, A., Salter, I., Schaber, M., Scholz, D., Soltwedel, T., Torres-Valdes, S., Wekerle, C., Wenzhöfer, F., Wietz, M., and Boetius, A.: Sea-ice derived meltwater stratification slows the biological carbon pump: results from continuous observations, Nature Communications, 12, 7309, https://doi.org/10.1038/s41467-021-26943-z, 2021.

Wadhams, P., Holfort, J., Hansen, E., and Wilkinson, J. P.: A deep convective chimney in the winter greenland sea, Geophysical Research Letters, 29, https://doi.org/10.1029/2001GL014306, 2002.

Wallace, D., Behrens, W., Hopkins, T., Kinder, C., Deming, J., Smith, W., Top, Z., and Walsh, I.: Collaborative research on the Northeast Water Polynya: NEWP92 hydrographic data report. USCGC Polar Sea cruise, July 15–August 15, 1992, Tech. Rep. BNL–61923, 102497, https://doi.org/10.2172/102497, 1995a.

Wallace, D. W. R., Minnett, P. J., and Hopkins, T. S.: Nutrients, oxygen, and inferred new production in the Northeast Water Polynya, 1992, Journal of Geophysical Research, 100, 4323, https://doi.org/10.1029/94JC02203, 1995b.

Willcox, E. W., Bendtsen, J., Mortensen, J., Mohn, C., Lemes, M., Pedersen, T.-J., Holding, J., Møller, E. F., Sejr, M. K., Seidenkrantz, M.-S., and Rysgaard, S.: An Updated View of the Water Masses on the Northeast Greenland Shelf and Their Link to the Laptev Sea and Lena River, Journal of Geophysical Research: Oceans, 128, e2022JC019 052, https://doi.org/10.1029/2022JC019052, 2023.

Yager, P. L., Wallace, D. W. R., Johnson, K. M., Smith, W. O., Minnett, P. J., and Deming, J. W.: The Northeast Water Polynya as an atmospheric CO_2 sink: A seasonal rectification hypothesis, Journal of Geophysical Research, 100, 4389, https://doi.org/10.1029/94JC01962, 1995.

Yasunaka, S., Siswanto, E., Olsen, A., Hoppema, M., Watanabe, E., Fransson, A., Chierici, M., Murata, A., Lauvset, S. K., Wanninkhof, R., Takahashi, T., Kosugi, N., Omar, A. M., van Heuven, S., and Mathis, J. T.: Arctic Ocean CO2 uptake: an improved multiyear estimate of the air–sea CO2 flux incorporating chlorophyll a concentrations, Biogeosciences, 15, 1643–1661, https://doi.org/10.5194/bg-15-1643-2018, 2018.

Zeebe, R. E. and Wolf-Gladrow, D. A.: CO_2 in seawater: equilibrium, kinetics, isotopes, no. 65 in Elsevier oceanography series, Elsevier, Amsterdam ; New York, 2001.

Zhuang, Y., Jin, H., Cai, W.-J., Li, H., Jin, M., Qi, D., and Chen, J.: Freshening leads to a three-decade trend of declining nutrients in the western Arctic Ocean, Environmental Research Letters, 16, 054 047, https://doi.org/10.1088/1748-9326/abf58b, 2021.

Zhuang, Y., Jin, H., Cai, W.-J., Li, H., Qi, D., and Chen, J.: Extreme Nitrate Deficits in the Western Arctic Ocean: Origin, Decadal Changes, and Implications for Denitrification on a Polar Marginal Shelf, Global Biogeochemical Cycles, 36, e2022GB007 304, https://doi.org/10.1029/2022GB007304, 2022.

Supplement with CO_2 paper

AUTHORS

Contents

Goal of this supplement 1

Water mass fractions on the shelf 2

Salinity normalisation of carbonate chemistry 5

Modified Z-scores 8

Comparison with SOCAT and CARINA data 8

References 10

Goal of this supplement

The ability of the ocean to dissolve carbon dioxide (CO_2) gas is primarily affected by temperature, salinity, the buffer capacity of the ocean (measured as titrated alkalinity) and the amount of total dissolved inorganic carbon (the sum of all inorganic carbon species in solution once released as CO_2 gas and measured by coulometric titration). To analyse the carbon chemistry from bottle data they are commonly normalised to remove the effect of salinity (S) (Broecker and Peng 1992; Friis, Körtzinger, and Wallace 2003; Yamamoto-Kawai, Tanaka, and Pivovarov 2005) or temperature (Takahashi et al. 2002, 2009). This allows the analysis of the influence of other processes on the carbon system. Generally, the four main abiotic influences on the carbonate system are temperature, salinity, total alkalinity (TA), and dissolved inorganic carbon (DIC) where the TA is generally considered to be conservative with salinity and the DIC is influenced primarily by autotrophic production and remineralisation (Zeebe and Wolf-Gladrow 2001). When normalising data with respect to salinity in environments where TA is conservative with salinity, analyses can focus on the biology. For surface water transported to higher latitudes from low and mid latitudes, the increase in gas solutbility is is associated with the decrease in temperature (Li and Tsui 1971; Weiss 1970; Millero 2013). For an isochemical water mass, the relationship was established by Takahashi et al. (1993) to be ($\partial \ln pCO_2/\partial T$) = 0.0423 ± 0.0002 °C^{-1} for water taken from the North Atlantic.

The Northeast Greenland shelf is a unique high latitude coastal environment with more possible influences on the carbonate system than in lower latitude open ocean environments. The environment can not be expected to be isochemical, nor is the surface water all cooled. Water found at the surface and originating in the Artic Ocean will be exposed to increasing atmospheric temperatures with decreasing latitude in summer which would reduce the solubility of CO_2, while the return Atlantic Water might either heat or cool depending on conditions on the eastern side of Fram Strait, the season during which it arrives on the shelf, and the amount of (melting) sea ice it encounters. Similarly, the other main variables measured to calculate the CO_2 have different sources or are subject to complex processes on the shelf.

This supplement is intended to highlight some details which are relevant to but not directly part of the study. The first is a discussion surrounding the use of water mass tracers on the Northeast Greenland shelf and the errors associated with it. The second is a justification for our choice of using a polynomial fit to normalise the data rather than using more common methods. Finally we provide some detail regarding our use of the modified Z-score, and a comparison between our data and that found in the SOCAT and CARINA databases.

Water mass fractions on the shelf

In an idealised estuarine environment there is a single freshwater source with which incoming ocean water is diluted. This source can be glacial or riverine, and precipitation is considered either negligible or as part of the same catchment. The TA of the freshwater source can be obtained by performing a linear regression between total alkalinity and salinity and finding the TA at S = 0. In a northern latitude fjord environment dilution of the surface layer by sea ice melt is an additional process. This makes the analysis more complex since sea ice retains TA in the form of the hydrated mineral ikaite ($CaCO_3 \cdot 6\,H_2O$) and so is no longer conservative with the salinity, both in the meltwater influenced layer as well as the underlying water into which the salty but TA-depleted water is mixed. In an idealised fjord with a single meteoric freshwater source and local sea ice formation and melting the sea ice melt influence can be approximated by performing a water mass fraction analysis. This is most frequently done by using a system of linear equations where 2 tracers are used to obtain 3 unknown water mass fractions . The most commonly used tracers are salinity and stable water oxygen isotopic composition ($\delta^{18}O$), which are independent from one another both for meteoric as well as sea ice freshwater sources, for end-members of Atlantic Water, Meteoric freshwater, and sea ice melt as shown in Equations 1, 2, and 3.

$$f_{sim} + F_{mw} + F_{aw} = 1 \tag{1}$$

$$\delta^{18}O_{sim} + \delta^{18}O_{mw} + \delta^{18}O_{aw} = \delta^{18}O_{obs} \tag{2}$$

$$S_{fsim} + S_{mw} + S_{aw} = S_{obs} \tag{3}$$

where subsripts sim, mw, and aw refer to sea ice melt, meteoric freshwater and Atlantic Water end members and obs to the observed (measured) values.

The Northeast Greenland shelf is not an idealised northern latitude fjord, it is a complex broad Arctic continental shelf which receives multiple advected watermasses and receives additional local inputs. The water advected onto the shelf is not a pure Atlantic Water end member, it is instead comprised of return Atlantic Water, directly from the West Spitsbergen Current and Eurasian Basin sourced Arctic Atlantic Water which is much colder and may have been subject to processes specific to the Arctic that the return current has not including such things as dense water cascades or sedimentary interactions.

The upper water which includes the cold halocline layer and the surface water is influenced by sea ice melt and by the input of 10-11% of global meteoric river discharge (Shiklomanov et al. 2021). Each of the 6 major rivers discharging into the Arctic Ocean has its own average TA and $\delta^{18}O$ values which also vary seasonally (Cooper et al. 2008), Due to these complexities we can't assume that TA is conservative with salinity.

The 3 linear equations & solve for 1 unknown system commonly used to determine the water mass fractions is sensitive to the choice of the salinity and $\delta^{18}O$ for sea ice. Sea ice $\delta^{18}O$ can vary depending on the water from which it was frozen, whether or not it is covered in snow, and on its age (first year versus multiyear ice) (Mellat et al. 2024). For end member values AW (S=35.0, $\delta^{18}O$=0.3‰), MW (S=0, $\delta^{18}O$=-20‰) and sea ice melt with S = 2 set to $\delta^{18}O$ of -4, -1, and 0.2‰ respectively entered into the system of linear equations, the lowest negative meteoric meltwater fraction (so an indicator of the size of the introduced error) in our data are -9.9%, -8.2%, -7.8% respectively. It is less sensitive to the salinity of the sea ice. For a $\delta^{18}O$ of 0.3‰ , S = 4 results in a maximum negative freshwater fraction of -7.7% and remains the same (when rounded to 2 significant figures) at S = 0.

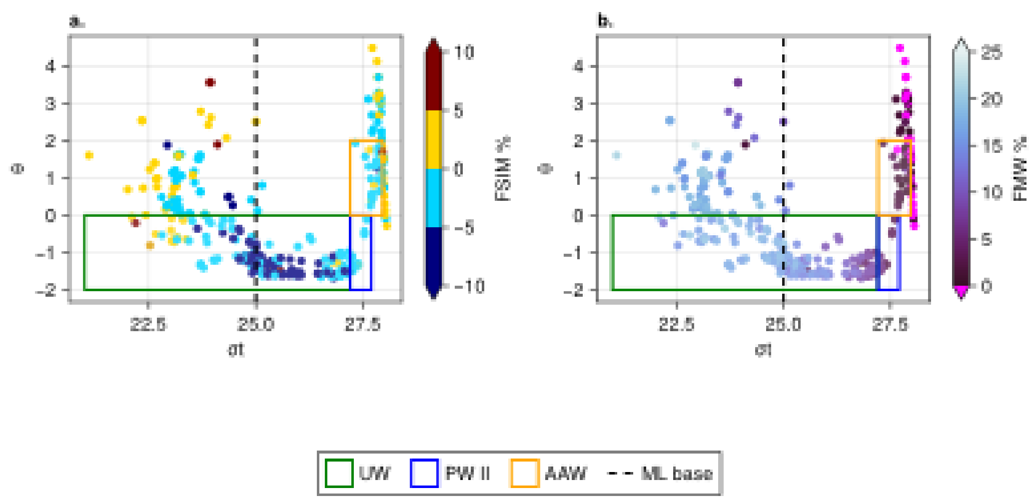

Figure 1: Density against temperature with fractions of sea ice melt (top) and meteoric water (bottom). Water mass boundaries (Rudels et al, 2022) in colour and the remnant of the winter mixed layer in the black dashed line. Acronyms UW is Upper Water, PW II is Polar Water 2 which refers to the lower halocline & winter mixed layer in the upstream Nansen Basin. Note that the Atlantic Water sea ice melt fraction is close to 0 while simultaneously, the upper water mixes from high in brine (negative melt) to high in sea ice melt crossing through 0 sea ice melt. Meteroic freshwater (FMW) has negative fractions, primarily at high densities which is clearly in error since meteoric freshwater input can't be negative. It is therefore apparent that the system of linear equations with which the water fractions are calculated is lacking the end-members or end-member values required to properly assign these fractions at each data point, likely due to the high variability of input sources

For representative end-member values of AW (S=35.0, $\delta^{18}O$=0.3 ‰), MW (S=0, $\delta^{18}O$=-20 ‰), and for SIM S=2 and the mean $\delta^{18}O$ value of sea ice collected and melted during the second cruise: $\delta^{18}O$ = -2.34 ‰ (Willcox et al. 2023). It can be seen that the Cold Halocline Layer (CHL, from the base of the winter mixed layer at σt=25 to the Polar Water II at σt=27.2) is most influenced by negative sea ice melt (generally interpreted as brine) and all other water, the more dense Polar II and Arctic Atlantic Water as well as the surface water have meltwater fractions of 0 ± 5 %. For the surface water this is not a problem since the meteoric freshwater and Atlantic Water fractions are not below 0. It does pose a problem for the higher density waters (σt > 27.2) where the freshwater and/or Atlantic Water fractions are unrealistically < 0 % (magenta in Figure fig. 1 b) and the sea ice meltwater fraction is lower than those erroneously negative fractions. When Atlantic Water enters the Arctic Ocean, it eventually forms the lower halocline when the warm water is rapidly cooled, by loss of heat to the atmosphere, but also through the melting of sea ice and a meltwater signature in these denser waters could be correct and can not be simply discarded. This issue can't be easily resolved without the use of additional tracers such as the ^{236}U and ^{129}I anthropogenic radionuclides which can differentiate between different Atlantic Waters based on their time spent in transit.

Table 1: End member values used to determine water mass fractions. Meteoric water values for $\delta^{18}O$ and TA are those of the Lena river according to (Cooper et al. 2008). Sea ice melt values for $\delta^{18}O$ and TA are from own measurements on the shelf

	Salinity	$\delta^{18}O$ (‰ VSMOW2)
Sea ice melt	2	-2.344 ± 0.746
Meteoric	0	-20.5
Atlantic	35.0	0.3

Salinity normalisation of carbonate chemistry

The TA of return Atlantic Water that has sea ice melted directly into it may be different (say a TA of 2330 diluted with a mean shelf sea ice concentration of ~204 µmol/kg) to the TA of Arctic Atlantic Water that has a similar salinity but may have had brine and meltwater added during multiple years spent in the Arctic Ocean. Simply correcting with the sea ice meltwater fraction therefore may not be sufficient to describe local processes.

The simplest formulation of the salinity normalisation of marine inorganic carbon system data is given by Equation eq. 4 where the reference salinity normalised to is often 35 (Peng et al. 1987). Several modifications to this have been proposed with time including those which involve corrections for nutrients (Broecker and Peng 1992).

$$nX = \frac{X_{meas}}{S_{meas}} \cdot S_{ref} \tag{4}$$

where X is the variable to be corrected for, e.g. TA and/or DIC, S is the salinity, and meas and ref subscripts stand for the field measurements and the reference value respectively.

Whether the resulting normalised data are entirely independent of freshwater flux has been questioned (Robbins 2001). Later iterations were developed specifically for higher latitudes including corrections for a TA estimated by linear regression at the point S = 0 (Friis, Körtzinger, and Wallace 2003), and for the calculated sea ice melt fraction (Yamamoto-Kawai, Tanaka, and Pivovarov 2005). Each of these corrections has associated issues and errors and may not provide useful information, especially where there are multiple low salinity sources for TA such as shelf environments host to catchments with differing geology. Although there is an official descriptions of what a reference salinity is (Wright et al. 2010), it is often either chosen to be 35 or a regionally obtained variable, often the mean salinity. This makes any comparison between different geographical regions with different dominant water masses and therefore chosen reference salinity for calculated values subject icomparable. This complexity primarily impacts mixed layer depths (Friis, Körtzinger, and Wallace 2003) where the meteoric-influenced layer is highest or multiple different sources such as precipitation, riverine inputs, and sea ice melt, contribute to the dilution. If these normalizations rely on other assumptions such as those underlying the calculation of sea ice melt fraction from δ^{18}O, any error in these assumptions will be propagated into any subsequent application using the normalized data.

The processes controlling the water mass composition and the associated shelf salinity and alkalinity are complex. In addition, fraction calculations suffer from the ambiguities discussed in the previous subsection, therefore these data might best be normalized with respect to salinity by the simple removal of a polynomial-predicted value from the data, rather than attempting to correct for the assumed representative values for the Northeast Greenland shelf which contains such vastly variable sources in unknown relative quantities.

For purposes of comparison and to choose the best representative method for the salinity normalisation of the carbonate system data, four different salinity corrections were applied (Figure 2). The first (Figure 2a) is the direct application of the polynomial in Equation 5:

$$X_{pred} = X_{obs} - X_{poly} + X_{meanS} \tag{5}$$

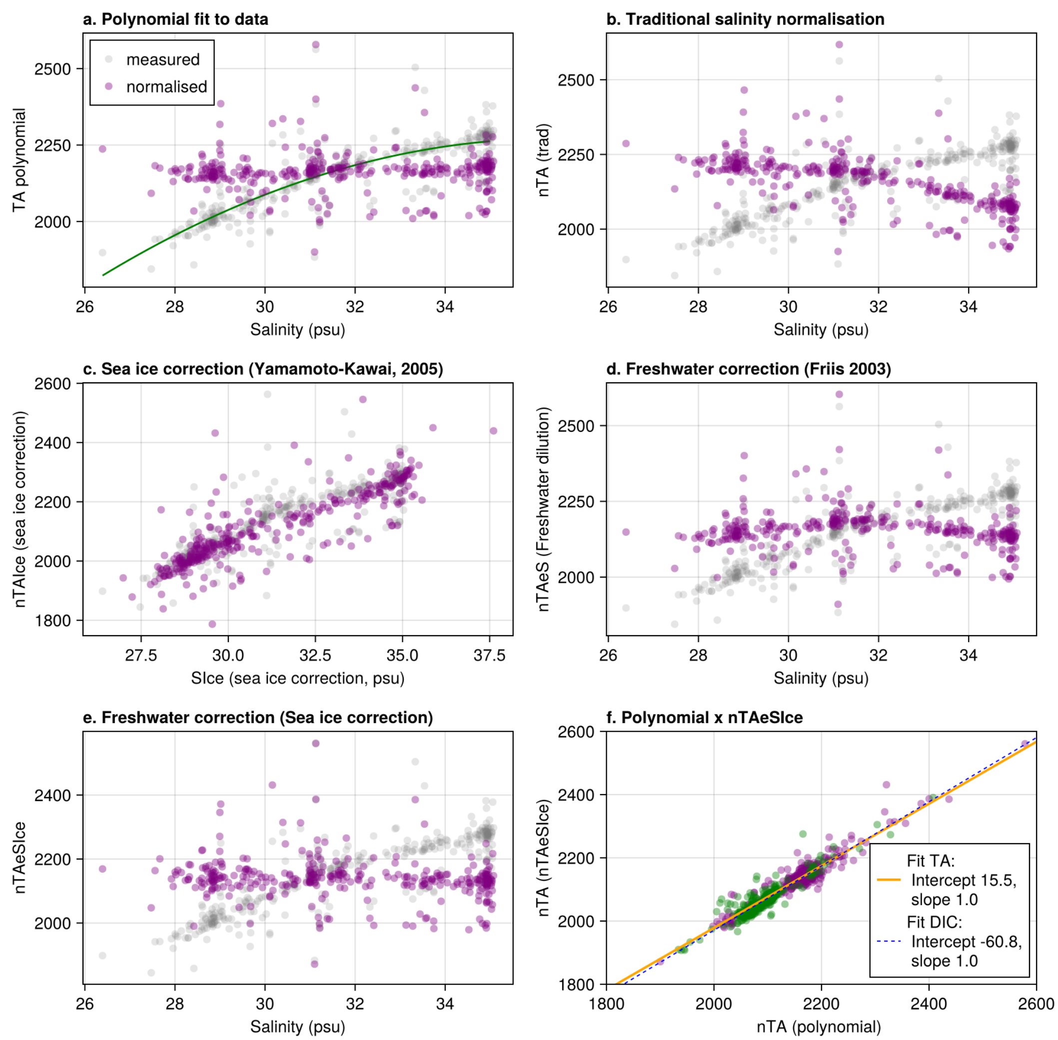

Figure 2: Comparison of normalisation techniques. Application by polynomial fit using the green line with equation TA = -3631.43 + 324.03 S - 4.45 S^2 (a), traditional salinity normalisation (b), Sea ice correction (c), Meteoric freshwater correction (d), Meterric correction applied to sea ice corrected data (e) and ~~finally~~ a comparison between sea ice + freshwater corrections and the polynomial correction indicating a slope of 1 between them

where pred is the salinity-normalised value estimated by the equation, obs is the observational data, poly is the value predicted by the polynomial fit (green line in Figure 2a), and X_{meanS} the mean salinity for the dataset. This method therefore still relies on an arbitrary choice of reference salinity but it reduces the number of assumptions made about external influences on the data such as the calculated fraction of sea ice melt although these have results that are comparable enough to be used interchangeably (Figure 2f).

Modified Z-scores

Modified Z-scores rely on the Absolute Median Deviation (MAD) rather than the mean of a dataset and thus allow for the labeling of outliers in datasets where the mean is too sensitive to outliers. This modified Z-score is calculkated according to Equations 6 and 7.

$$MAD = median_i(|x_i - \tilde{x}|) \tag{6}$$

$$M_i = \frac{0.6745(x_i - \tilde{x})}{MAD} \tag{7}$$

Data can then be flagged as an outlier if $|M_i| > D$. Although Iglewicz and Hoaglin (1993) suggest a D of 3.5, this doesn't adequately flag all outliers in our data. To make sure all outliers based on visual inspection are flagged as such we require D = 1.5.

Comparison with SOCAT and CARINA data

Limited Surface Ocean CO2 Atlas (SOCAT) carbon dioxide fugacity measurements and and full depth CARbon dioxide IN the Atlantic Ocean (CARINA) total alkalinity (TA) and dissolved inorganic carbon (DIC) data are available for the region of this study, however it is both geographically (Figure 1 a. main text) as well as temporally limited (Figure 4). For the time period (late August and September) of our study in late fall, there is only SOCAT data available from 2009 and CARINA data from 1994 and 2003 and therefore these data are not ideal for comparative purposes.

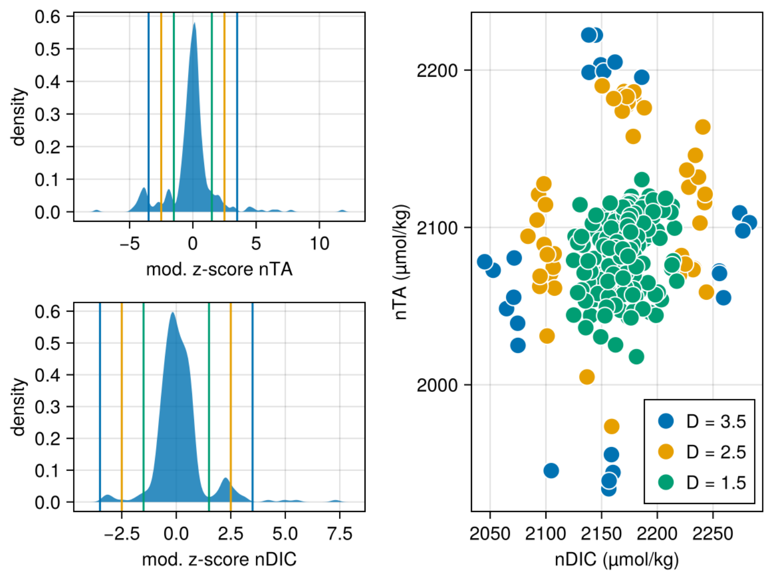

Figure 3: Density plots of the modified Z-scores of normalised TA and DIC (a,b) and of the data not flagged as outliers based on different choice of D

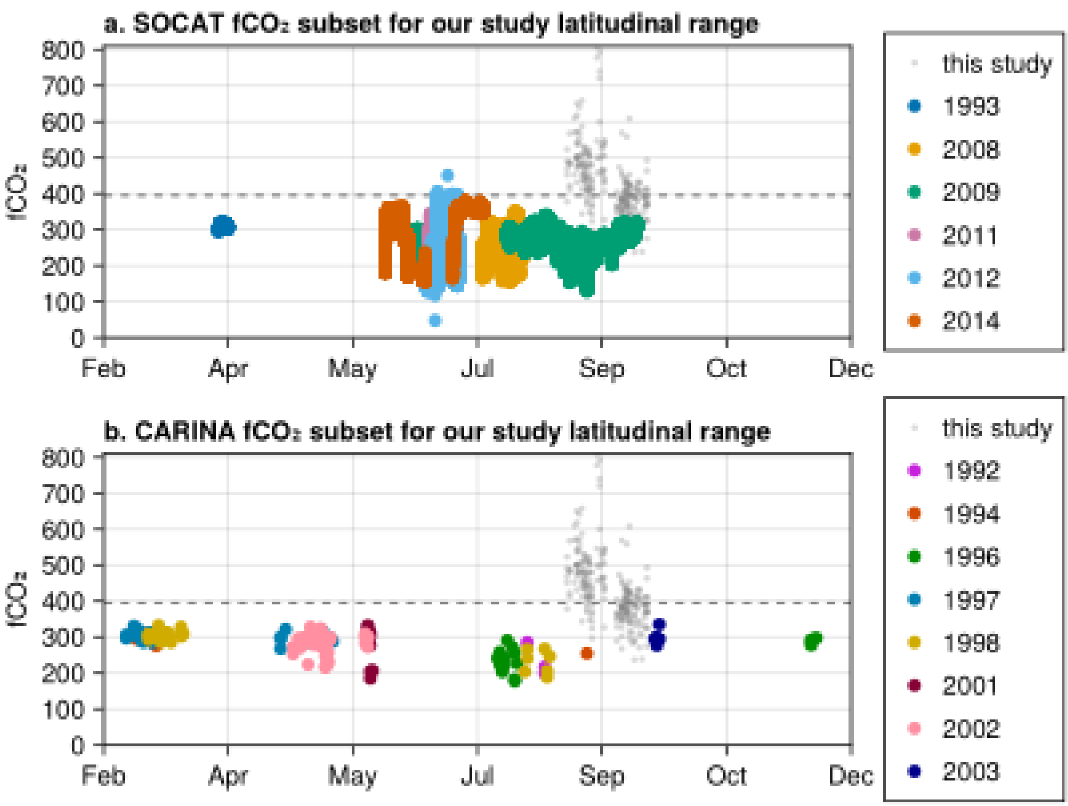

Figure 4: SOCAT measured fCO_2 (a) and CARINA CO2SYS calculated fCO_2 (b) for geographical area on and around the Northeast Greenland shelf compared to data from our study where D = 1.5. The grey dashed line is at 395 µatm, which is representative for the time of our study per Fay et al. (2021)

References

Broecker, Wallace S., and Tsung-Hung Peng. 1992. "Interhemispheric Transport of Carbon Dioxide by Ocean Circulation." Nature 356 (6370): 587–89. https://doi.org/10.1038/356587a0.

Cooper, L. W., J. W. McClelland, R. M. Holmes, P. A. Raymond, J. J. Gibson, C. K. Guay, and B. J. Peterson. 2008. "Flow-Weighted Values of Runoff Tracers (d18O, DOC, Ba, Alkalinity) from the Six Largest Arctic Rivers." Geophysical Research Letters 35 (18): L18606. https://doi.org/10.1029/2008gl035007.

Fay, Amanda R., Luke Gregor, Peter Landschützer, Galen A. McKinley, Nicolas Gruber, Marion Gehlen, Yosuke Iida, et al. 2021. "SeaFlux: Harmonization of Air–sea CO2 Fluxes from Surface pCO2 Data Products Using a Standardized Approach." Earth System Science Data 13 (10): 4693–4710. https://doi.org/10.5194/essd-13-4693-2021.

Friis, K., A. Körtzinger, and D. W. R. Wallace. 2003. "The Salinity Normalization of Marine Inorganic Carbon Chemistry Data: THE SALINITY NORMALIZATION OF MARINE INORGANIC CARBON CHEMISTRY DATA." Geophysical Research Letters 30 (2). https://doi.org/10.1029/2002gl015898.

Iglewicz, Boris, and David C. Hoaglin. 1993. Volume 16: How to Detect and Handle Outliers. La Vergne: ASQ Quality Press.

Li, Yuan-Hui, and Tien-Fung Tsui. 1971. "The Solubility of CO_2 in Water and Sea Water." Journal of Geophysical Research 76 (18): 4203–7. https://doi.org/10.1029/JC076i018p04203.

Mellat, Moein, Camilla F. Brunello, Martin Werner, Dorothea Bauch, Ellen Damm, Michael Angelopoulos, Daiki Nomura, et al. 2024. "Isotopic Signatures of Snow, Sea Ice, and Surface Seawater in the Central Arctic Ocean During the MOSAiC Expedition." Elem Sci Anth 12 (1): 00078. https://doi.org/10.1525/elementa.2023.00078.

Millero, Frank J. 2013. Millero, Frank J - Chemical Oceanography, Fourth Edition-CRC Press (2013).pdf. Fourth. Boca Raton, FL: CRC Press.

Peng, Tsung-Hung, Taro Takahashi, Wallace S. Broecker, and Jon Olafsson. 1987. "Seasonal Variability of Carbon Dioxide, Nutrients and Oxygen in the Northern North Atlantic Surface Water: Observations and a Model*." Tellus B 39B (5): 439–58. https://doi.org/10.1111/j.1600-0889.1987.tb00205.x.

Robbins, Paul E. 2001. "Oceanic Carbon Transport Carried by Freshwater Divergence: Are Salinity Normalizations Useful?" Journal of Geophysical Research: Oceans 106 (C12): 30939–46. https://doi.org/10.1029/2000JC000451.

Shiklomanov, Alexander, Stephen Déry, Mikhail Tretiakov, Daqing Yang, Dmitry Magritsky, Alex

Georgiadi, and Wenqing Tang. 2021. "River Freshwater Flux to the Arctic Ocean." In Arctic Hydrology, Permafrost and Ecosystems, edited by Daqing Yang and Douglas L. Kane, 703–38. Cham: Springer International Publishing. https://doi.org/10.1007/978-3-030-50930-9$_%7B2 %7D$4.

Takahashi, Taro, Jon Olafsson, John G. Goddard, David W. Chipman, and S. C. Sutherland. 1993. "Seasonal Variation of CO_2 and Nutrients in the High-Latitude Surface Oceans: A Comparative Study." Global Biogeochemical Cycles 7 (4): 843–78. https://doi.org/10.1029/93GB02263.

Takahashi, Taro, Stewart C. Sutherland, Colm Sweeney, Alain Poisson, Nicolas Metzl, Bronte Tilbrook, Nicolas Bates, et al. 2002. "Global Sea–air CO2 Flux Based on Climatological Surface Ocean pCO2, and Seasonal Biological and Temperature Effects." Deep Sea Research Part II: Topical Studies in Oceanography 49 (9-10): 1601–22. https://doi.org/10.1016/s0967-0645(02)00003-6.

Takahashi, Taro, Stewart C. Sutherland, Rik Wanninkhof, Colm Sweeney, Richard A. Feely, David W. Chipman, Burke Hales, et al. 2009. "Climatological Mean and Decadal Change in Surface Ocean pCO2, and Net Sea–air CO2 Flux over the Global Oceans." Deep Sea Research Part II: Topical Studies in Oceanography 56 (8-10): 554–77. https://doi.org/10.1016/j.dsr2.2008.12.009.

Weiss, R. F. 1970. "The Solubility of Nitrogen, Oxygen and Argon in Water and Seawater." Deep Sea Research and Oceanographic Abstracts 17 (4): 721–35. https://doi.org/10.1016/0011-7471(70)90037-9.

Willcox, E. W., J. Bendtsen, J. Mortensen, C. Mohn, M. Lemes, T.-J. Pedersen, J. Holding, et al. 2023. "An Updated View of the Water Masses on the Northeast Greenland Shelf and Their Link to the Laptev Sea and Lena River." Journal of Geophysical Research: Oceans 128 (4): e2022JC019052. https://doi.org/10.1029/2022JC019052.

Wright, D. G., R. Pawlowicz, T. J. McDougall, R. Feistel, and G. M. Marion. 2010. "Absolute Salinity, &Quot;Density Salinity" and the Reference-Composition Salinity Scale: Present and Future Use in the Seawater Standard TEOS-10." Preprint. All Depths/Operational Oceanography/All Geographic Regions/Temperature, Salinity; Density Fields. https://doi.org/10.5194/osd-7-1559-2010.

Yamamoto-Kawai, Michiyo, Noriyuki Tanaka, and Sergey Pivovarov. 2005. "Freshwater and Brine Behaviors in the Arctic Ocean Deduced from Historical Data of δ18O and Alkalinity (1929–2002 A.D.)." Journal of Geophysical Research: Oceans 110 (C10). https://doi.org/10.1029/2004JC002793.

Zeebe, Richard E., and Dieter A. Wolf-Gladrow. 2001. CO_2 in Seawater: Equilibrium, Kinetics, Isotopes. Elsevier Oceanography Series 65. Amsterdam ; New York: Elsevier.